

In situ X-ray pair distribution function analysis of accelerated carbonation of a synthetic calcium-silicate- hydrate gel

Antoine E. Morandea^a, Claire E. White^{a*}

^a Department of Civil and Environmental Engineering and the Andlinger Center for Energy
and the Environment, Princeton University, Princeton NJ, USA

Supplementary Information

X-ray Data Collection and Analysis

Immediately prior to the X-ray PDF measurement, the as-synthesised C-S-H gel was dried on a hot plate at 60°C for 30 min in order to reduce the overall H₂O content of the gel. Initial measurements of the C-S-H gel using X-ray PDF analysis revealed that the data were dominated by the water-containing atom-atom correlations due to a relatively large amount of adsorbed water in the sample. Hence, the drying process was included in order to reduce the overall content of adsorbed water. Subsequent comparisons of the atomic ordering of this C-S-H gel with gels analysed in the literature in the past using X-ray PDF analysis revealed that the drying process did not adversely affect the atomic structure of the gel.^{1,2}

It should be mentioned that the CO₂ concentration of the flow gas was chosen based on the fact that this investigation centres on the assessment of the viability of using X-ray PDF analysis to study the carbonation reaction in real time, and therefore 100% CO₂ was utilised in order to ensure that full carbonation was achieved for the C-S-H gel. It is known that this high concentration of CO₂ will impact the reaction kinetics and development of specific crystalline calcium carbonate polymorphs,^{3,4} and therefore this was taken into account throughout the analysis and discussion of the data.

Reciprocal Space Analysis

For this investigation, a nickel calibration sample was used in order to obtain the instrument parameters using a pseudo-Voigt profile function.⁵ C-S-H gel was modelled in reciprocal-space using the recent C-S-H structure file produced by Battocchio et al.⁶ (ICSD #187041) with a Ca/Si=1.14. The sample also contained varying amounts of the crystalline calcium carbonate polymorphs: calcite⁷ (ICSD #18166) and vaterite^{8,9} (COD #913565) as the carbonation reaction progressed. The scale factors of C-S-H gel, calcite and vaterite were refined in order to quantify the evolution of these phases as an extent of the carbonation reaction, and therefore to obtain information on the kinetics of reaction with respect to a particular phase (i.e., C-S-H gel, calcite and vaterite). The weighted profile R-factor R_{wp} is presented in Fig. S.1.

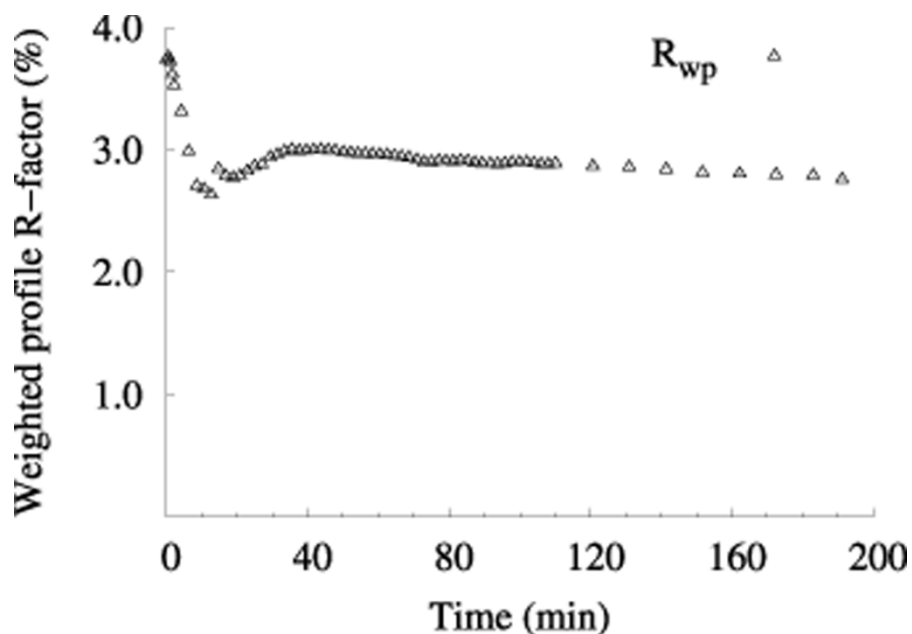


Figure S.1. Weighted profile R-factor R_{wp} for the Rietveld refinement as a function of the carbonation time.

Real Space Analysis: Calcite and Vaterite Refinement

Results of the refinement of calcite and vaterite fitted to the fully-carbonated PDF data set (after 3 hrs of carbonation) are given in Table S.1. The empirical correction for the nearest-neighbour correlation (δ_2) was not refined due to the high r region over which parameters were being fitted. Instead, this parameter was manually adjusted to account for the entire C-O correlation (fixed at 1.5), and this value was kept fixed when the calcite and vaterite contributions were removed from the carbonated C-S-H gel PDF data set.

Table **Error! No sequence specified.**: PDF refined parameters for calcite and vaterite after 3 hrs of carbonation over an r range of 40 to 65 Å. The level of agreement obtained for this refinement was $R_w = 0.23$ (R_w defined in PDFgui¹⁰). Units for the lattice parameters (a , b and c) are given in Å and for the atomic displacement parameters (u_i) in Å².

	Calcite	Vaterite
$a = b$	4.99170	7.15256
c	17.06007	25.39381
u_i (Ca)	0.0049	0.0088
u_i (C)	0.0053	0.0128
u_i (O)	0.0116	0.0342

Once accurate simulated PDFs of calcite and vaterite were obtained, the C-S-H gel/amorphous silica gels for the other PDF data sets throughout the carbonation reaction were obtained using a purpose designed least-squares method (using Matlab) to subtract out the calcite and vaterite contributions. The terms that were allowed to change in order to obtain the best fit with the experimental data (at high r) were the scale factors for calcite and vaterite (S_{calcite} and S_{vaterite} , respectively, see Eq. (1)). The residual PDF at low r (< 40 Å) denoted as $G(r)_{\text{am}}$ in Eq. (S.1) is the remaining C-S-H/amorphous gel in the sample.

$$G(r)_{\text{am}} = G(r) - (S_{\text{calcite}} G(r)_{\text{calcite}} + S_{\text{vaterite}} G(r)_{\text{vaterite}}) \quad (\text{S.1})$$

Real space analysis: Structure of C-S-H gel

Prior to analysing the real space data as a function of the carbonation reaction, it is necessary to ensure that the double decomposition method used to synthesise the C-S-H gel in this investigation has produced an atomic structure of C-S-H gel that is in agreement with previous results available in the literature. Fig. S.2 displays the X-ray PDF obtained for the synthetic C-S-H gel studied in this investigation together with the experimental results obtained by White et al.² for synthetic C-S-D gels (where D stands for deuterated water). These gels by White et al. were synthesised via hydration of tricalcium silicate (C_3S) mixed with various amounts of silica fume in order to obtain different Ca/Si ratios. The gels displayed in Fig. S.2 from the investigation by White et al. are those for nanocrystalline C-S-D gel after the removal of (i) unreacted crystalline C_3S and (ii) crystalline calcium hydroxide from the measured X-ray PDF data.² The peaks located at r values below $\sim 1.2 \text{ \AA}$ in Fig. S.2 are artefacts and are due to imperfect corrections and termination errors.¹¹

Despite the difference in the method of synthesis for the gels, the short range order seen in Fig. S.2 is very similar irrespective of the synthesis method. This is particularly evident via comparison of the Si-O and Ca-O atom-atom correlations, where the Ca/Si ratio of the double-decomposition C-S-H gel produced in this investigation falls between that for the two C-S-D gels, which have Ca/Si ratios of 0.57 and 0.93. Furthermore, the medium range ($> 3 \text{ \AA}$) and long range ($> 7 \text{ \AA}$) ordering for the C-S-H gel are very similar to that of the C-S-D gel with a Ca/Si ratio of 0.57. This agreement, together with the results from previous PDF experiments showing C-S-H gels are nanocrystalline^{1,2} proves that the double decomposition method is successful in replicating the local atomic structure and nanocrystalline nature of this important OPC phase.

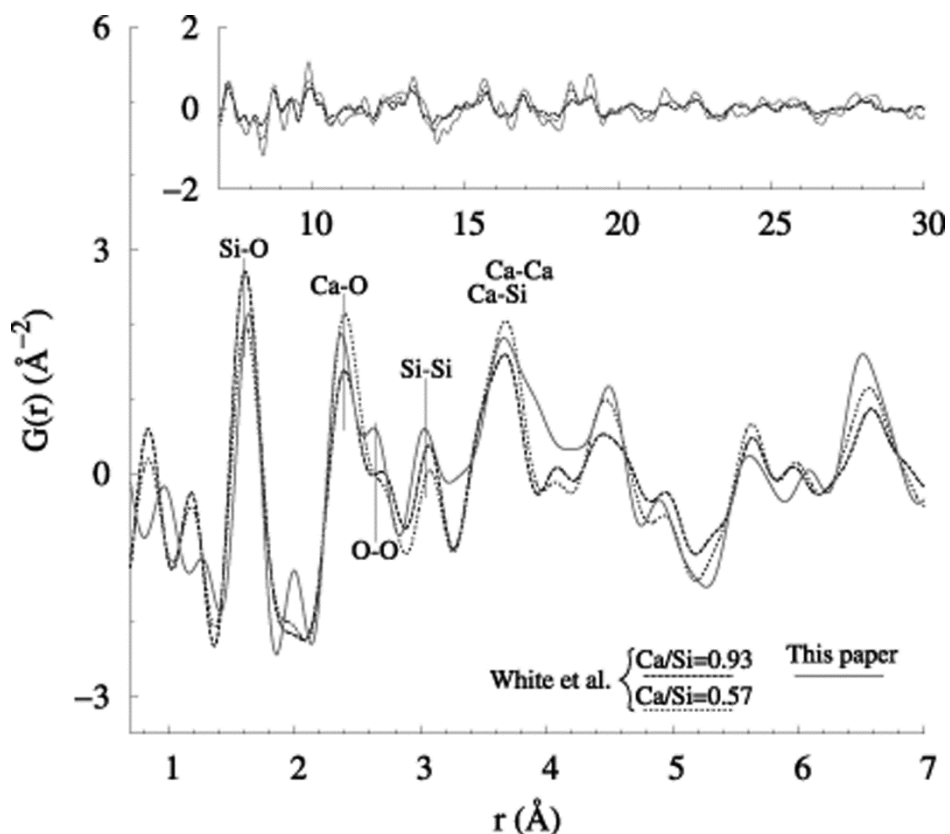


Figure S.2. Comparison of the initial X-ray PDF for C-S-H gel analysed in this investigation with the X-ray PDF of two C-S-D gels presented by White et al.² Peak assignments are given based on reference^{12,13}.

It is important to note that there are evident differences visible in Fig. S.2 for the gels synthesised via different methods. Possible reasons for this disagreement could include the slight differences in Ca/Si ratios, where the ratio for our C-S-H gel was determined to be 1.4 via XRF analysis. Furthermore, as seen in the previous section of this investigation, the C-S-H gel sample does contain a small percentage of crystalline calcite, which will contribute to the local structural ordering present in Fig. S.2. This crystalline contribution will also influence the longer range ordering, and therefore explains the increase in some of the atom-atom correlation intensities

seen in Fig. S.2 between 10 and 30 Å. Lastly, the water content of the gels may be different, which would lead to differences in the atom-atom correlations containing water molecules. This is most noticeable via the O-O correlation at ~ 2.8 Å, which may be an indication that the C-S-H gel synthesised via the double-decomposition method has a higher water content compared to those from the investigation by White et al.²

References

1. L. B. Skinner, S. R. Chae, C. J. Benmore, H. R. Wenk and P. J. M. Monteiro, *Phys. Rev. Lett.*, 2010, **104**, 195502.
2. C. E. White, L. L. Daemen, M. Hartl and K. Page, *Cem. Concr. Res.*, 2015, **67**, 66–73.
3. N. Hyvert, A. Sellier, F. Duprat, P. Rougeau and P. Francisco, *Cem. Concr. Res.*, 2010, **40**, 1582–1589.
4. S. A. Bernal, J. L. Provis, D. G. Brice, A. Kilcullen, P. Duxson and J. S. J. van Deventer, *Cem. Concr. Res.*, 2012, **42**, 1317–1326.
5. R. A. Young and D. B. Wiles, *J. Appl. Crystallogr.*, 1982, **15**, 430–438.
6. F. Battocchio, P. J. M. Monteiro and H.-R. Wenk, *Cem. Concr. Res.*, 2012, **42**, 1534–1548.
7. H. Chessin, W. C. Hamilton and B. Post, *Acta Crystallogr.*, 1965, **18**, 689–693.
8. J. Wang, F. Zhang, J. Zhang, R. C. Ewing, U. Becker and Z. Cai, *J. Cryst. Growth*, 2014, **407**, 78–86.
9. J. Wang and U. Becker, *Am. Mineral.*, 2009, **94**, 380–386.
10. C. L. Farrow, P. Juhas, J. W. Liu, D. Bryndin, E. S. Bozin, J. Bloch, T. Proffen and S. J. L. Billinge, *J. Phys. Condens. Matter*, 2007, **19**, 335219.
11. T. Egami and S. J. L. Billinge, *Underneath the Bragg Peaks: Structural Analysis of Complex Materials*, Pergamon, Elmsford NY, 2003.

12. F. M. Michel, J. MacDonald, J. Feng, B. L. Phillips, L. Ehm, C. Tarabrella, J. B. Parise and R. J. Reeder, *Chem. Mater.*, 2008, **20**, 4720–4728.
13. C. Meral, C. J. Benmore and P. J. M. Monteiro, *Cem. Concr. Res.*, 2011, **41**, 696–710.